Ecological Indicators 103 (2019) 542–553

Contents lists available at ScienceDirect

Ecological Indicators

journal homepage: www.elsevier.com/locate/ecolind

Quantitative analysis of the contributions of climatic and human factors to grassland productivity in northern China

Yuchao Yan[a], Xiaoping Liu[a,*], Youyue Wen[b], Jinpei Ou[a]

[a] Guangdong Key Laboratory for Urbanization and Geo-simulation, School of Geography and Planning, Sun Yat-sen University, Guangzhou 510275, PR China
[b] South China Institute of Environmental Science, MEP, NO. 18 Ruihe RD., Guangzhou 510535, PR China

ARTICLE INFO

Keywords:
Climate change
Human activities
Grassland productivity
NPP
Quantitative analysis

ABSTRACT

An accurate quantitative analysis of the contributions of climate change (CC) and human activities (HA) to grassland productivity is crucial for elucidating the relevant driving mechanisms. In this study, grassland in northern China was analyzed. We chose the net primary productivity (NPP) as an evaluation indicator of grassland productivity and identified the relative roles of climatic and human factors in NPP changes. A quantitative method based on partial derivatives was used for evaluating the contributions of climatic factors to NPP changes, and the difference between the inter-annual variation rate of NPP and climatic factors contribution was considered as the HA contribution. Then, different scenarios were designed to evaluate the relative contribution proportions of CC and HA to grassland restoration and degradation. The results revealed that the average grassland NPP over northern China showed a significant increasing trend at a rate of 1.66 g C m^{-2} $year^{-1}$ from 2000 to 2015. The contributions of temperature, precipitation, and solar radiation to grassland NPP changes were 0.06, 0.50, and 0.52 g C m^{-2} $year^{-1}$, respectively. Solar radiation made the greatest positive contribution among all of the climatic factors, followed by precipitation. The contributions of CC and HA to grassland NPP changes were 1.08 and 0.58 g C m^{-2} $year^{-1}$, respectively. Moreover, the role of HA in both grassland restoration and degradation was larger than that of CC. Overall, the positive effect of HA on grassland productivity may be greatly offset by its negative effect, and therefore the positive contribution of HA to grassland NPP changes was less than that of CC. Thus, the effective measures and policies used to control grassland degradation should be further strengthened to protect grassland resources.

1. Introduction

Global climate change (CC) has been seriously influenced by the increased atmospheric CO_2 concentration (Joos et al., 2001; Keenan et al., 2012). Terrestrial ecosystem, which dominates the inter-annual variations of atmospheric CO_2 concentration, plays an important function in sequestering carbon (Huang et al., 2016). As a key component of the terrestrial ecosystem, grassland is one of the most common vegetation types, covering approximately 25% of the earth's terrestrial area (Liu et al., 2019). Grassland ecosystems are among the very important terrestrial carbon pools and hold approximately 20% of the global carbon storage (Chen et al., 2016; Scurlock and Hall, 1998), and thus play an irreplaceable role in mitigating greenhouse gas concentrations and maintaining climate stability.

Furthermore, grassland net primary productivity (NPP), which refers to the rate of net carbon fixed through photosynthesis by grassland, directly reflects the production capacity of grassland in the natural environment and is an important indicator of grass growth and dynamics (Field et al., 1998; Lieth and Whittaker, 2012; Potter et al., 1993). It is widely known that grassland NPP changes are easily affected by CC and human activities (HA) (Chen et al., 2014; Zhou et al., 2014; Zhou et al., 2017), and consequently it is necessary to assess the relative roles of CC and HA to further discern the dynamic mechanisms of grassland productivity. However, because of the complexity of the driving mechanisms, it is difficult to identify the contributions of climatic and human factors.

In the past, studies have attempted to quantitatively evaluate the contributions of CC and HA to ecosystems by using mathematical statistical methods (e.g., regression analysis and principal component analysis) (Du et al., 2014; Gollnow and Lakes, 2014; Newman et al., 2014; Schweizer and Matlack, 2014). The contributions of specific factors (e.g., temperature, precipitation, income, technology, and population) can be obtained by using these methods, but which ignore the ecological processes and cannot obtain the difference in the spatial

* Corresponding author.
E-mail address: liuxp3@mail.sysu.edu.cn (X. Liu).

https://doi.org/10.1016/j.ecolind.2019.04.020
Received 30 December 2018; Received in revised form 31 March 2019; Accepted 9 April 2019
Available online 22 April 2019

distribution of each factor's contribution. Other studies have used the residuals trend of the NDVI (RESTREND) method to investigate the contributions of CC and HA to land degradation (Herrmann et al., 2005; Jiang et al., 2017). The main idea of this method is that the correlated relationships between vegetation and precipitation is constructed to predict the NDVI, and the difference between the predicted and observed NDVI is considered as the impact of HA. However, this method is primarily applicable to arid and semi-arid zones, where precipitation has a strong impact on the vegetation growth (Wessels et al., 2007). Moreover, many studies have employed the dynamics of potential NPP and the difference between the potential and actual NPP to distinguish the influences of CC and HA on grassland (Chen et al., 2014; Wang et al., 2016; Zhou et al., 2014; Zhou et al., 2017), desertification (Li et al., 2016; Xu et al., 2010; Zhou et al., 2015), marsh (Mao et al., 2014), and urban eco-environments (Wu and Wu, 2018). However, the potential NPP is a virtual value with great uncertainty, and the contribution of single driving factor associated with CC and HA cannot be estimated by using this method. Therefore, to overcome the drawbacks of previous methods, this study tries to propose an improved method for quantitatively analyzing the contributions of climatic and human factors to grassland productivity.

In China, grassland is mostly distributed in the north, including northern temperate and Tibetan Plateau regions, which account for 78% of all Chinese grassland area (Chen and Wang, 2000). Grassland resources not only contribute substantially to milk and meat production (Liu et al., 2019), but also play an important role in preventing desertification and sand storms, conserving soil and water, and maintaining biodiversity (Costanza et al., 1997). As a result of global warming, dramatic changes in land use, and population growth (Harris, 2010; Kang et al, 2007; Nan, 2005), approximately 90% of Chinese grasslands have been degraded to varying degrees (Zhou et al., 2014; Wang et al., 2016). Grassland degradation has generated many serious environmental problems, such as desertification, dust sandstorms, soil erosion, and loss of biodiversity (Kang et al, 2007; Zhou et al., 2014; Zhou et al., 2017). To resolve these problems, a series of ecological restoration projects have been implemented by the Chinese government to control grassland degradation, such as the Grain to Green Program (GTGP, which was initiated in 1999 to return cropland to forest and grassland in ecologically fragile regions) and the Grazing Withdrawal Program (GWP, which was initiated in 2003 to protect grassland resources by banning grazing, rest grazing, and rotational grazing) (Zhang et al., 2016; Zhou et al., 2014; Zhou et al., 2017). The effects of these projects have led to substantial concerns among the population.

Against this background, the relative roles that CC and HA played in northern China's grassland productivity were evaluated. The specific objectives were as follows: (1) to evaluate the temporal-spatial dynamics of grassland productivity; (2) to establish a method for quantitatively analyzing the contributions of climatic and human factors to grassland NPP changes; and (3) to explore different scenarios in which CC and HA contributed to grassland restoration and degradation. These findings will provide a theoretical reference for policy makers aiming to optimize ecosystem management and achieve the sustainable use of grassland resources.

2. Materials and methods

2.1. Study area

The study area includes several provinces of northern China and the Tibetan Plateau (26°07′–53°30′ N; 73°50′–125°88′ E). Northern provinces include Gansu (GS), Shaanxi (SAX), Shanxi (SX), Hebei (HB), Inner Mongolia (IM), Ningxia (NX), and Xinjiang (XJ) (Fig. 1). The grasslands in these provinces are mainly located in arid and semi-arid areas, characterized by a dry climate and little rain. The provinces in the Tibetan Plateau include Qinghai (QH), Tibet (TB), and the west of Sichuan (SC) (Fig. 1). Because of the high altitude (more than 4000 m), the Tibetan Plateau has a typical plateau mountain climate, also known as an alpine climate, characterized by a relatively low mean temperature and large differences between daytime and nighttime temperatures. The grassland area of these provinces in the study area account for 96.79% of the total grassland area in China. There are many grassland types such as alpine meadow, alpine steppe, alpine desert-steppe, temperate meadow-steppe, temperate steppe, and montane meadow distributed within the study area. In the current context of climate change and human intervention, the study area has experienced serious grassland degradation and desertification.

2.2. Data sources and processing

2.2.1. Datasets for the Carnegie-Ames-Stanford Approach (CASA) model

The global land cover products were obtained from the European Space Agency (ESA) Climate Change Initiative Land Cover (CCI-LC) product. The spatial resolution of these data is 300 m × 300 m. The spatial distribution of grassland in northern China was extracted from global land cover data by using the vector boundary of the study area.

The 250-m 16-day composite Moderate Resolution Imaging Spectroradiometer (MODIS) vegetation indices (MOD13Q1) were provided by the United States Geological Survey (USGS). The maximum value composite (MVC) algorithm was applied on the original NDVI time series to construct monthly NDVI datasets, which were then resampled to a spatial resolution of 300 m × 300 m.

Meteorological data in the study area and nearby provinces from 2000 to 2015, including monthly mean temperature, monthly total precipitation, and monthly total solar radiation, were downloaded from the Chinese Meteorological Administration (CMA). Temperature and precipitation data were collected at 370 meteorological stations, and solar radiation data were retrieved from 75 stations. To ensure the consistency and continuity of data, any suspicious or missing records were screened and eliminated. To match the spatial resolution of the land cover and NDVI datasets, all meteorological datasets were interpolated at a spatial resolution of 300 m × 300 m by using ANUSPLIN software under consideration of latitude, longitude, and elevation.

The soil map originating from the Harmonized World Soil Database (HWSD) was used to obtain the soil textures (including fraction of sandy/silt/clay for top- and sub-soil layers). These determine the soil water-holding ability and are required parameters for driving the CASA model.

2.2.2. Measurement data

To validate the grassland NPP estimated from the CASA model, we sampled 135 sites in early April and late July of 2013 and 2014. At each sampling site (10 m × 10 m), we set up four quadrats (5 m × 5 m) and marked them as S_1, S_2, S_3, and S_4, respectively. At each quadrat, we collected grass from five smaller plots (1 m × 1 m). To calculate the annual NPP, we sampled each quadrat twice. The first sampling was S_1 and S_3 in early April and the second sampling was S_2 and S_4 in late July. To measure the aboveground biomass, all the grass in each plot was carefully clipped to ground level (Fig. 2b). To measure the underground biomass, nine soil cores (10 cm diameter) were collected from 0 to 60 cm depth at 10 cm intervals at each quadrat (Fig. 2c). In the laboratory, the root samples were first placed in a mesh sieve and then immersed in deionized water to remove soil residue and gravel. The biomass samples were dried at 65 °C to constant weight using an oven. Biomass was converted to carbon content by multiplying by a conversion coefficient of 0.45 (Fang et al., 2007). The annual grassland NPP was calculated by the difference between the maximum carbon content (measured in late July) and the minimum carbon content (measured in early April).

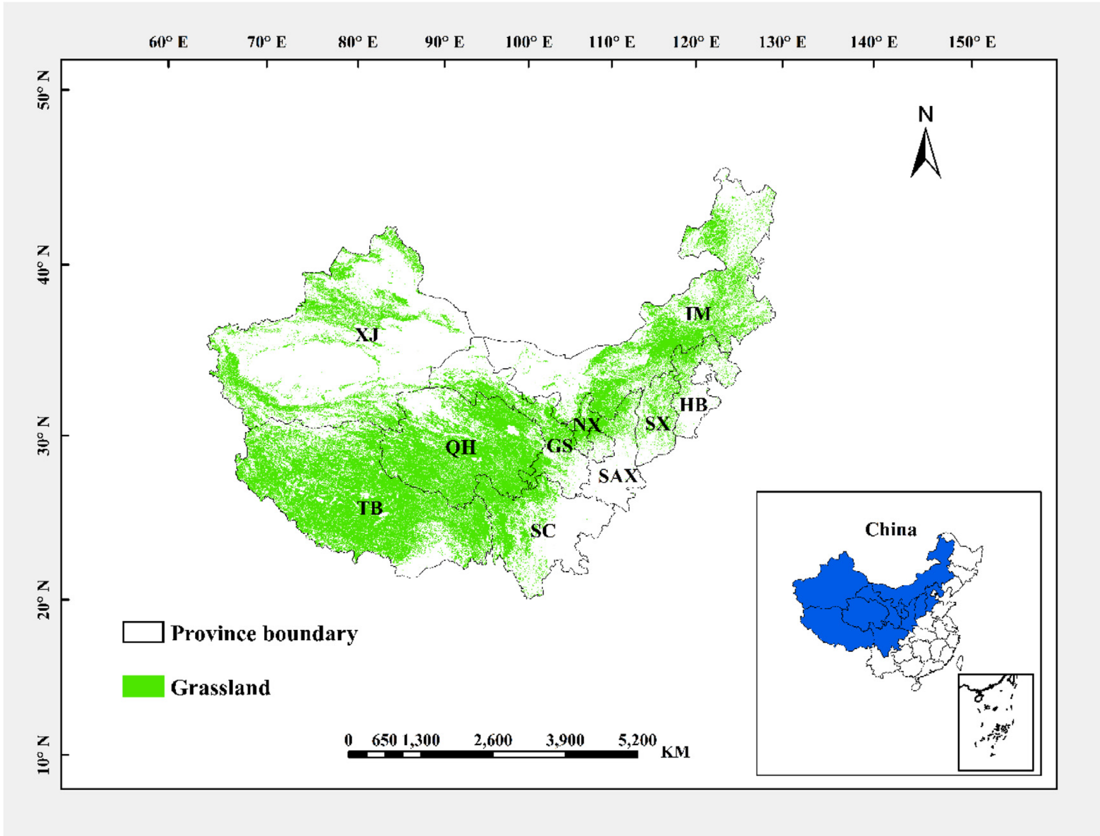

Fig. 1. Location of the study area.

2.3. Methods

2.3.1. CASA model for the calculation of NPP

The CASA model was driven by the NDVI, temperature, precipitation, solar radiation, land use/land cover, and soil property data. The formula is as follow:

$$NPP = 0.5 \times SOL \times FPAR \times T_1 \times T_2 \times W_s \times \varepsilon_{max} \quad (1)$$

where the coefficient of 0.5 is the fraction of active incoming solar radiation (wavelength 0.4–0.7 μm) utilized by vegetation; SOL ($MJ\,m^{-2}$) represents the total solar radiation; FPAR represents the fraction of photosynthetically active radiation absorbed by vegetation, which is a function of NDVI; T_1 (°C) denotes the limitation of extreme high and low temperature on light use efficiency (LUE) ($g\,C\,MJ^{-1}$); T_2 (°C) reflects the LUE ($g\,C\,MJ^{-1}$) when the temperature is higher or lower than the optimal temperature throughout the year; $W_s$is the moisture pressure on vegetation growth, which is a function of temperature, precipitation, and soil texture data; and ε_{max} ($g\,C\,MJ^{-1}$) is the maximum LUE for plants under the optimal living conditions. The result of Pei et al. (2013) was adopted here for the ε_{max}value of grassland in China. The detailed calculation steps for each parameter were documented by Potter et al. (1993).

To validate the CASA model, a comparative analysis of the simulated NPP with measured data was conducted. As shown in Fig. 3, the correlation analysis between estimated and measured NPP showed a good agreement, with a strong linear correlation ($R^2 = 0.726$, $P < 0.001$), which indicates that the grassland NPP in northern China was accurately estimated by the CASA model.

2.3.2. Assessment of the change trends of NPP and climatic factors

The ordinary least squares method was employed to conduct a linear regression of variables in the time dimension in order to analyze the temporal dynamics of NPP and climatic factors:

$$S = \frac{n \times \sum_{i=1}^{n} i \times Var_i - \sum_{i=1}^{n} Var_i \sum_{i=1}^{n} i}{n \times \sum_{i=1}^{n} i^2 - \left(\sum_{i=1}^{n} i\right)^2} \quad (2)$$

where S is the inter-annual variation rate of NPP or climatic factors; n is the study period, from 2000 to 2015; i is the sequence number of the year; and Var_i represents the research variables in year i, including NPP, temperature, precipitation, and solar radiation. Taking the variation trend of NPP for example, a positive S indicates that NPP shows an increasing trend over time and vice versa.

Fig. 2. Field sampling of grassland in northern China: (a) setting the small plot; (b) clipping the grass to ground level; and (c) acquiring the soil cores.

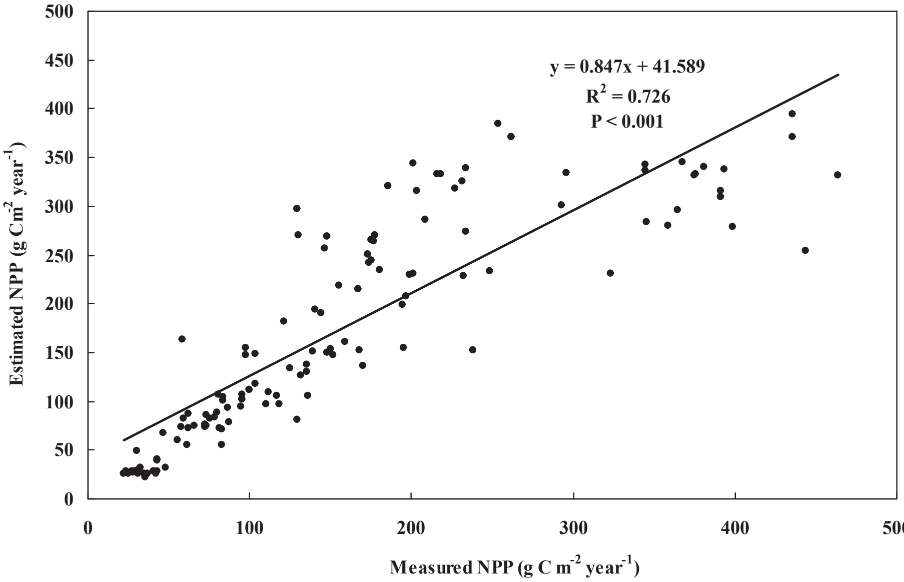

Fig. 3. Comparison of the estimated NPP with measured data.

2.3.3. Partial correlation analysis between NPP and climatic factors

Partial correlation analysis is an effective measurement for studying the linear relationship between two factors while removing the effects of one or more interferential factors (Xu, 2006). This approach has been widely used by many previous studies to explore the relationship between vegetation growth and a single climatic factor (Peng et al., 2013; Wu et al., 2015; Wen et al., 2018). The partial correlation coefficients between NPP and different climatic factors were analyzed as follows:

$$R_{xy,z} = \frac{R_{xy} - R_{xz} * R_{yz}}{\sqrt{(1 - R_{xz}^2) * (1 - R_{yz}^2)}} \tag{3}$$

where $R_{xy,z}$ is the partial correlation coefficient between x and y in the case of removing the effect of variable z; x, y, and z represent the independent variable, dependent variable, and control variable, respectively; R_{xy}, R_{xz}, and R_{yz} are the simple correlation coefficients between x, y, z.

Taking R_{xy} as an example, the correlation coefficients between NPP and climatic factors were calculated by the following formula:

$$R_{xy} = \frac{\sum_{i=1}^{n} (x_i - \bar{x})(y_i - \bar{y})}{\sqrt{\sum_{i=1}^{n} (x_i - \bar{x})^2}\sqrt{\sum_{i=1}^{n} (y_i - \bar{y})^2}} \tag{4}$$

where R_{xy} is the simple correlation coefficient between x and y; n = 16 years; x_i is the annual average temperature, annual total precipitation, or annual total solar radiation in a given year; $\bar{x}$ is the average value of temperature, precipitation, or solar radiation for 2000–2015; y_i is the NPP in a given year; and $\bar{y}$ is the average value of the NPP for 2000–2015.

2.3.4. Quantitative assessment of the contributions of climatic and human factors to NPP changes

On the basis of Roderick et al. (2007), Eq. (5), which is based on partial derivatives and has been widely employed to evaluate the impacts of various climatic factors on evaporation or hydrological changes (Liu and Sun, 2016; Meng and Mo, 2012; Yang and Yang, 2012; You et al., 2013), was attempted to be used for assessing the contribution of each driving factor to NPP changes:

$$\frac{dY}{dt} = \varepsilon_{X_1}\frac{dX_1}{dt} + \varepsilon_{X_2}\frac{dX_2}{dt} + \varepsilon_{X_3}\frac{dX_3}{dt} + \cdots + \varepsilon_{X_n}\frac{dX_n}{dt} = X_{1\_con} + X_{2\_con} + X_{3\_con} + \cdots + X_{n\_con} \tag{5}$$

where X_{1_con}, X_{2_con}, X_{3_con}, …, and X_{n_con} represent the contributions of X_1, X_2, X_3, …, and X_n to Y variations, respectively. The elastic coefficients ε_{X_1}, ε_{X_2}, ε_{X_3}, …, and ε_{X_n} can be calculated as $\frac{\partial Y}{\partial X_1}$, $\frac{\partial Y}{\partial X_2}$, $\frac{\partial Y}{\partial X_3}$, …, and $\frac{\partial Y}{\partial X_n}$.

This study assumed that the grassland NPP changes was mainly influenced by CC and HA. Thus, Eq. (5) can also be described as:

$$S \approx C_{\_con} + H_{\_con} = Tem_{\_con} + Pre_{\_con} + Rad_{\_con} + H_{\_con} = \frac{\partial NPP}{\partial Tem} \times \frac{dTem}{dt} + \frac{\partial NPP}{\partial Pre} \times \frac{dPre}{dt} + \frac{\partial NPP}{\partial Rad} \times \frac{dRad}{dt} + H_{\_con} \tag{6}$$

where S is the inter-annual variation rate of the NPP; $C_{\_con}$, $H_{\_con}$, $Tem_{\_con}$, $Pre_{\_con}$, and $Rad_{\_con}$ represent the contributions of CC, HA, temperature, precipitation, and solar radiation to the inter-annual NPP changes, respectively; $C_{\_con}$ is the sum of $Tem_{\_con}$, $Pre_{\_con}$, and $Rad_{\_con}$; and $H_{\_con}$ is approximately equal to the residual between S and $C_{\_con}$. Moreover, $\frac{\partial NPP}{\partial Tem}$ is equal to the partial correlation coefficient between NPP and temperature when removing the disturbances of precipitation and solar radiation; $\frac{dTem}{dt}$ is the inter-annual variation rate of temperature; and $Tem_{\_con}$ is calculated as the product of $\frac{\partial NPP}{\partial Tem}$ and $\frac{dTem}{dt}$. A similar method is also suitable for $Pre_{\_con}$ and $Rad_{\_con}$. In this study, CO_2 fertilization, which has been shown to have a strong impact on the carbon sink in China (Mu et al., 2008), is included in HA. However, it has the weakest impact on grassland because only 0.3% of the total NPP of the Chinese grasslands was influenced by CO_2 fertilization (Mu et al., 2008). Rodents and pests greatly accelerated grassland degradation in China (Zhang, 2003). Because overgrazing is the main cause of grassland rodent damage and the harms of rodents and pests can be controlled by human management (Fang, 2013; Kang et al, 2007; Zhang et al., 2016), so this factor can be included in HA. Meanwhile, the impacts of grassland type and soil texture on grassland NPP changes can be neglected because their impacts were relatively constant within the study period (Zhang et al., 2016). Overall, HA can be assumed to play a dominant role in the remaining factors.

2.3.5. Scenarios for evaluating the contribution proportions of CC and HA to grassland restoration or degradation

Traditionally, an increase in NPP has been used as an indicator of vegetation restoration, whereas a decrease in NPP represents vegetation degradation (Xu et al., 2010; Zhang et al., 2016; Zhou et al., 2014; Zhou et al., 2015). Based on Eq. (2), a positive S in NPP represents grassland restoration, whereas a negative S denotes grassland degradation. The

Table 1
Six scenarios for quantifying the contribution proportions of CC and HA to grassland restoration and degradation.

	Scenario	$C_{\_con}$	$H_{\_con}$	Contribution proportion of CC (%)	Contribution proportion of HA (%)
$S > 0$	1	> 0	> 0	$\frac{\lvert C\_con \rvert}{\lvert C\_con \rvert + \lvert H\_con \rvert} \times 100$	$\frac{\lvert H\_con \rvert}{\lvert C\_con \rvert + \lvert H\_con \rvert} \times 100$
	2	> 0	< 0	100	0
	3	< 0	> 0	0	100
$S < 0$	1	< 0	< 0	$\frac{\lvert C\_con \rvert}{\lvert C\_con \rvert + \lvert H\_con \rvert} \times 100$	$\frac{\lvert H\_con \rvert}{\lvert C\_con \rvert + \lvert H\_con \rvert} \times 100$
	2	< 0	> 0	100	0
	3	> 0	< 0	0	100

positive $C_{\_con}$ and $H_{_con}$represent CC and HA that benefit grass growth, whereas the negative $C_{\_con}$ and $H_{\_con}$ represent CC and HA that hinder grass growth. Furthermore, six scenarios were designed in Table 1 based on S, $C_{\_con}$, and $H_{\_con}$ to assess the contribution proportions of CC and HA to grassland restoration and degradation.

In this study, when the contribution proportion of CC to grassland restoration or degradation was larger than that of HA, it was defined as “climate-dominated restoration or degradation”. Similarly, when the contribution proportion of HA to grassland restoration or degradation was greater than that of CC, it was defined as “human-dominated restoration or degradation”.

3. Results

3.1. Analysis of grassland NPP

3.1.1. Spatial distribution of NPP

The mean grassland NPP value in northern China during 2000–2015 was 242.02 g C m^{-2} year^{-1} (Fig. 5). The spatial distribution of mean grassland NPP value is shown in Fig. 4. Overall, the NPP value decreased markedly from the southeast to the northwest of the study area. More specifically, the province with the highest NPP value was observed in SC (545.52 g C m^{-2} year^{-1}, Fig. 5) in the southeast of the study area. Conversely, the NPP value reached the lowest level in XJ (137.24 g C m^{-2} year^{-1}, Fig. 5) in the northwest of the study area.

3.1.2. Temporal-spatial dynamics of NPP

The annual grassland NPP changes in northern China exhibited a significant increasing trend (1.66 g C m^{-2} year^{-1}, $P < 0.001$) from 2000 to 2015 (Table 2). Despite this overall increase, the spatial distribution of the change trend in grassland NPP showed clear regional differences (Fig. 6). The NPP increased in 64.94% of the grassland area (Fig. 6a), and the significant increasing trend ($P < 0.05$) accounted for 20.74% of this area (Fig. 6b). In contrast, NPP in 35.06% of the grassland area exhibited a decreasing trend (Fig. 6a). The area with a significant decreasing trend ($P < 0.05$) in NPP was very small and only accounted for 3.68% of the grassland area (Fig. 6b). Moreover, as shown in Table 2, the increasing trends of NPP in SAX (10.26 g C m^{-2} year^{-1}, $P < 0.001$), SX (10.21 g C m^{-2} year^{-1}, $P < 0.001$), HB (5.34 g C m^{-2} year^{-1}, $P < 0.001$), GS (3.65 g C m^{-2} year^{-1}, $P < 0.001$), IM (3.34 g C m^{-2} year^{-1}, $P < 0.01$), and NX (4.80 g C m^{-2} year^{-1}, $P < 0.001$) were statistically significant. However, in SC (2.10 g C m^{-2} year^{-1}, $P > 0.05$), QH (1.20 g C m^{-2} year^{-1}, $P > 0.05$), TB (−0.56 g C m^{-2} year^{-1}, $P > 0.05$), and XJ (1.19 g C m^{-2} year^{-1}, $P > 0.05$), the change trend in NPP were not statistically significant. In comparison, SAX showed the largest increasing trend in NPP, followed by SX.

3.2. Contributions of climatic and human factors to grassland NPP changes

Partial correlation analysis was performed to measure the

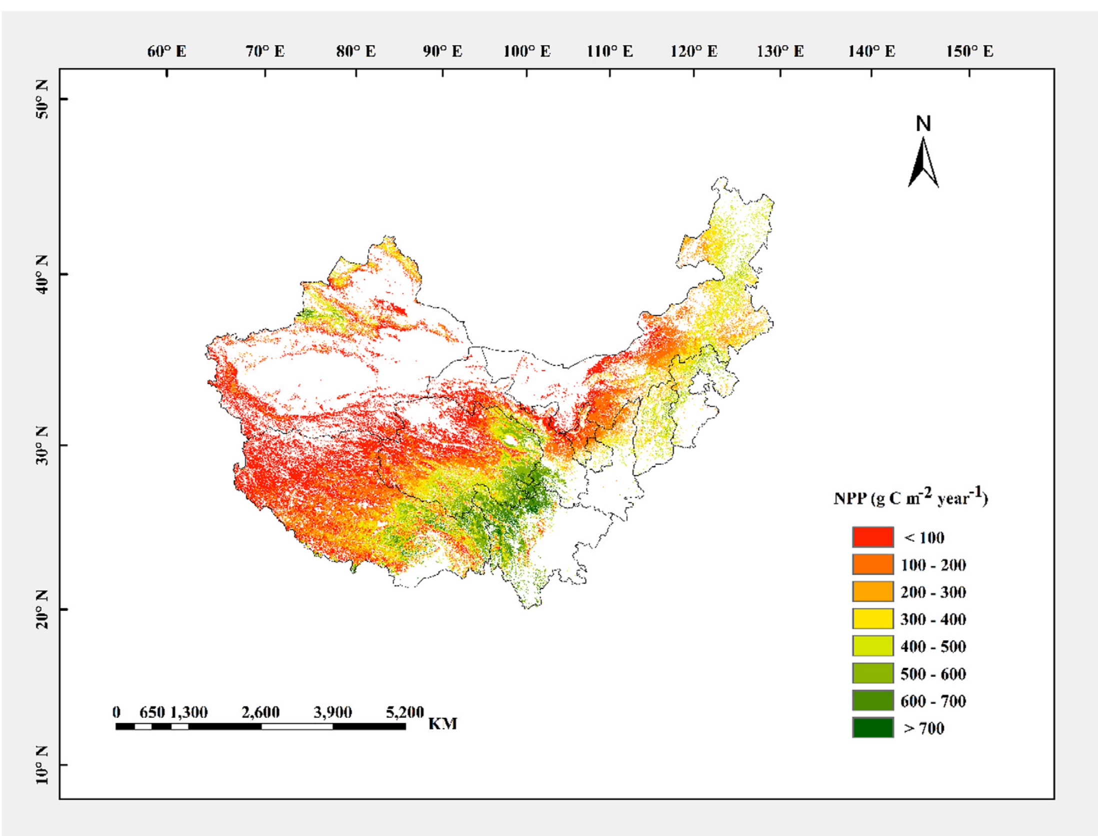

Fig. 4. Spatial distribution of mean grassland NPP value in northern China from 2000 to 2015.

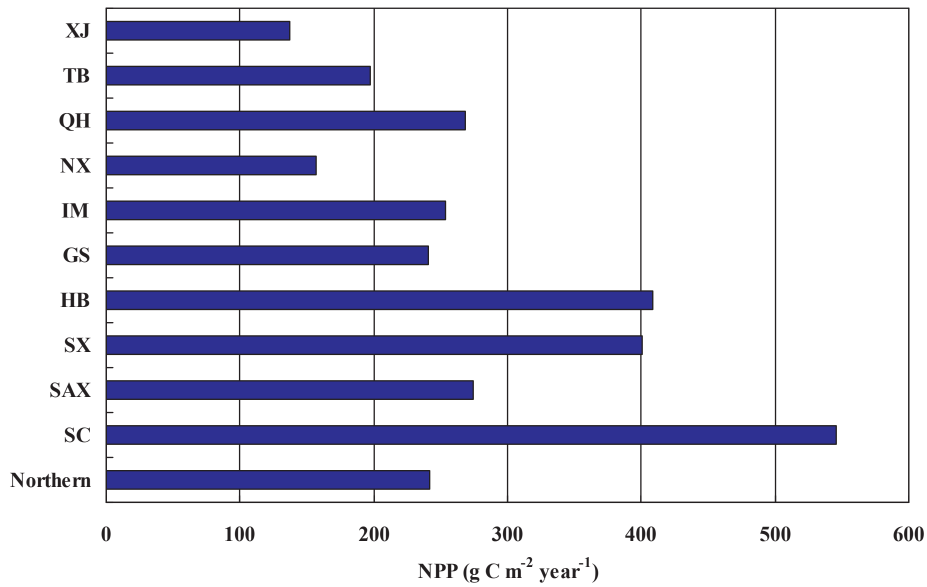

Fig. 5. Statistical analysis of grassland NPP value. See Fig. 1 for definitions of each province abbreviation.

Table 2
Statistical analysis of annual grassland NPP changes ($g\,C\,m^{-2}\,year^{-1}$). See Fig. 1 for definitions of each province abbreviation.

Regions	NPP changes	Regions	NPP changes
Northern	1.66^{***}	IM	3.34^{**}
SC	2.10	NX	4.80^{***}
SAX	10.26^{***}	QH	1.20
SX	10.21^{***}	TB	−0.56
HB	5.34^{***}	XJ	1.19
GS	3.65^{***}		

Notes: $^{***}P < 0.001$, $^{**}P < 0.01$, $^{*}P < 0.05$.

interactions between grassland NPP and climatic factors (Supplementary material). The partial correlation coefficient can describe the degree of correlation between grassland NPP and climatic factors, whereas the contributions of climatic factors to grassland NPP changes cannot be quantified. Therefore, to quantitatively evaluate the contributions of climatic factors to NPP changes, the results of Tem_con, Pre_con, and Rad_con are shown in Fig. 7. According to the statistical analysis (Table 3), from 2000 to 2015, the contributions of temperature, precipitation, and solar radiation to grassland NPP changes in northern China were 0.06, 0.50, and 0.52 $g\,C\,m^{-2}\,year^{-1}$, respectively. Solar radiation made the greatest positive contribution among all of the climatic factors, followed by precipitation, whereas temperature made the smallest positive contribution. Solar radiation made a greater positive contribution than temperature or precipitation in many provinces, including SC, SAX, SX, HB, GS, and XJ, and precipitation made a greater positive contribution than temperature or solar radiation in IM, NX, and QH. Among the different provinces, temperature, precipitation, and solar radiation made the greatest positive contributions to grassland NPP changes in SC (0.81 $g\,C\,m^{-2}\,year^{-1}$), IM (2.11 $g\,C\,m^{-2}\,year^{-1}$), and SX (5.36 $g\,C\,m^{-2}\,year^{-1}$), respectively. Both temperature and precipitation made the greatest negative contributions in TB (−0.23 and −0.28 $g\,C\,m^{-2}\,year^{-1}$). Solar radiation made the greatest negative contributions in QH (−0.12 $g\,C\,m^{-2}\,year^{-1}$).

Furthermore, the results of Tem_con, Pre_con, and Rad_con were used to obtain the contributions made by CC and HA (Fig. 8). The statistical results in Table 3 show that both CC and HA made positive contributions to grassland NPP changes in northern China, and CC

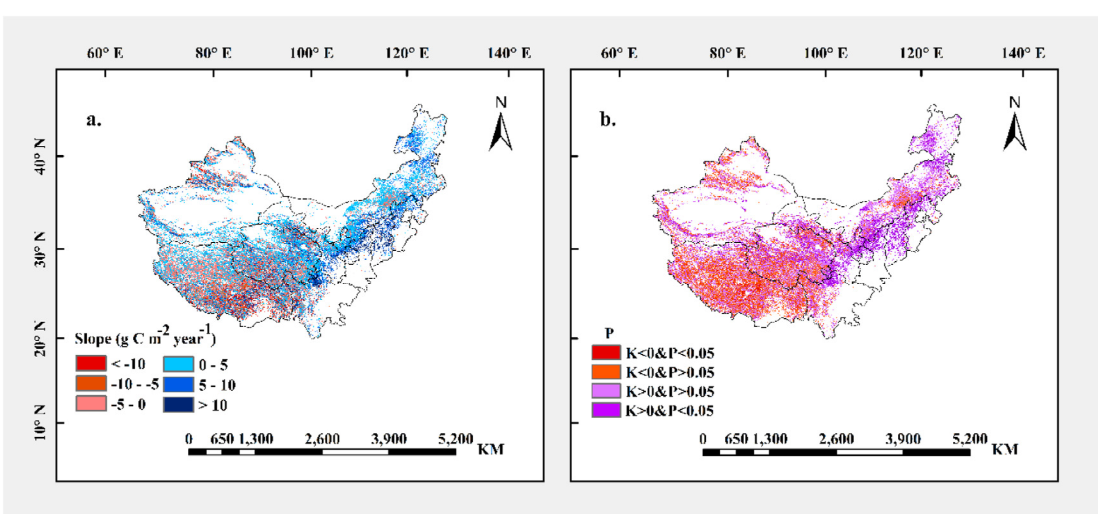

Fig. 6. Spatial distributions of (a) the change trend in grassland NPP and (b) the levels of significance.

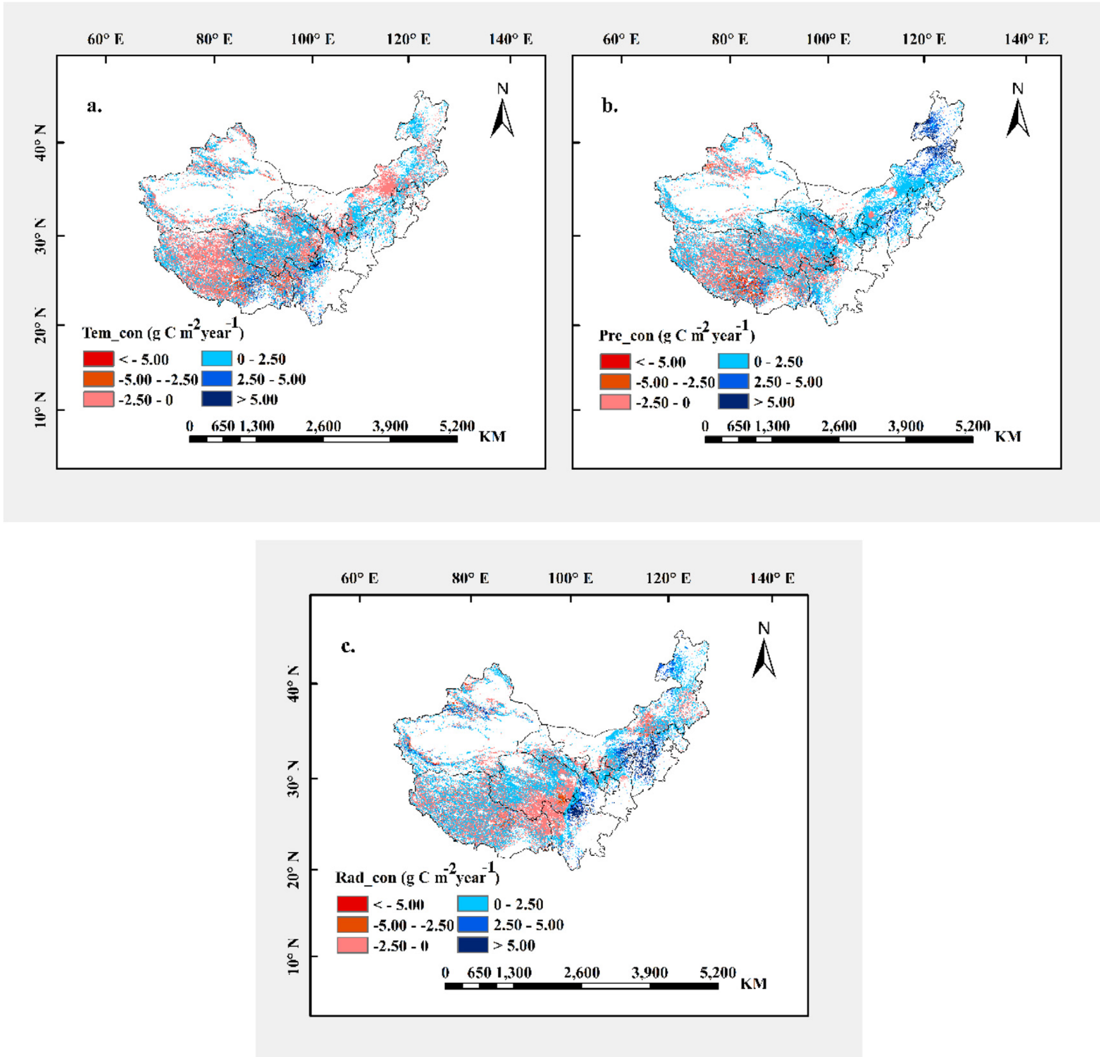

Fig. 7. Spatial distributions of the contributions of (a) temperature (Tem_con), (b) precipitation (Pre_con), and (c) solar radiation (Rad_con) to grassland NPP changes.

Table 3
Statistical analysis of the contributions of climatic and human factors to grassland NPP changes ($g\,C\,m^{-2}\,year^{-1}$). See Fig. 1 for definitions of each province abbreviation.

Regions	Temperature	Precipitation	Solar radiation	CC	HA
Northern	0.06	0.50	0.52	1.08	0.58
SC	0.81	0.14	1.35	2.30	−0.20
SAX	0.59	1.67	2.11	4.37	5.89
SX	0.23	1.79	5.36	7.38	2.83
HB	0.11	1.33	1.97	3.41	1.93
GS	0.24	0.50	1.00	1.74	1.91
IM	0.06	2.11	1.00	3.17	0.17
NX	0.08	1.30	0.15	1.53	3.27
QH	0.21	0.38	−0.12	0.47	0.73
TB	−0.23	−0.28	−0.05	−0.56	0.00
XJ	0.05	0.05	0.50	0.60	0.59

($1.08\,g\,C\,m^{-2}\,year^{-1}$) made a greater positive contribution than HA ($0.58\,g\,C\,m^{-2}\,year^{-1}$). CC and HA made a positive contribution in most provinces. CC made the greatest positive contribution in SX ($7.38\,g\,C\,m^{-2}\,year^{-1}$) then SAX ($4.37\,g\,C\,m^{-2}\,year^{-1}$), and HA made the greatest positive contribution in SAX ($5.89\,g\,C\,m^{-2}\,year^{-1}$) then NX ($3.27\,g\,C\,m^{-2}\,year^{-1}$). Conversely, CC and HA made the greatest negative contribution in TB ($-0.56\,g\,C\,m^{-2}\,year^{-1}$) and SC ($-0.20\,g\,C\,m^{-2}\,year^{-1}$), respectively.

3.3. Contribution proportions of CC and HA to grassland restoration or degradation

On the basis of the different scenarios designed in Table 1, the contribution proportions of CC and HA to grassland restoration and degradation were assessed (Figs. 9 and 10). The areas of climate- and human-dominated restoration and degradation (Fig. 11) were determined based on Figs. 9 and 10. Moreover, the results for the statistical analysis were acquired according to the area (Fig. 11) and annual grassland NPP changes (Fig. 6a). The area can reflect the scope of grassland productivity affected by CC and HA, and the NPP changes can reflect the changes of carbon sequestration in grassland. Thus, the results from the comprehensive statistical analysis based on the product of the area and NPP changes were of great use for determining the dominant factor to grassland restoration or degradation (Fig. 12).

As shown in Fig. 12a, the percentage of human-dominated restoration was larger than that of climate-dominated restoration (55.79% *vs.* 44.21%), and thus the impact of HA on grassland restoration was larger than that of CC in northern China. In addition, different results were observed in different provinces. First, the impact of CC on grassland restoration was larger than that of HA in SC (61.68% *vs.*

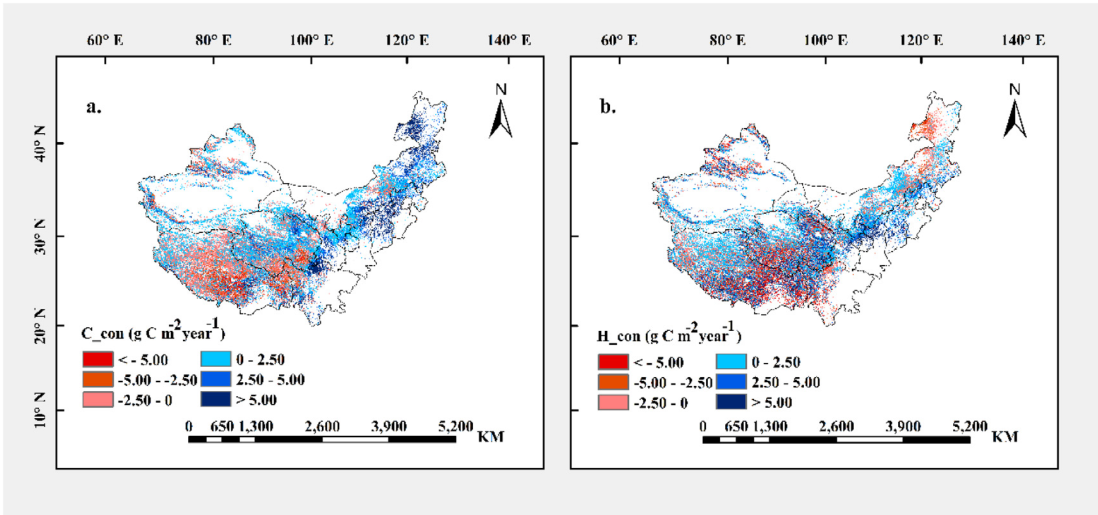

Fig. 8. Spatial distributions of the contributions of (a) CC (C_con) and (b) HA (H_con) to grassland NPP changes.

38.32%), SX (86.86% *vs.* 13.14%), HB (67.57% *vs.* 32.43%), and IM (80.09% *vs.* 19.91%). Second, the effect of HA on grassland restoration was larger than that of CC in the majority of provinces, including SAX (65.09% *vs.* 34.91%), GS (67.58% *vs.* 32.42%), NX (90.18% *vs.* 9.82%), QH (75.85% *vs.* 24.15%), TB (83.12% *vs.* 16.88%), and XJ (71.56% *vs.* 28.44%).

Meanwhile, as shown in Fig. 12b, the percentage of human-dominated degradation was larger than that of climate-dominated degradation in northern China (74.83% *vs.* 25.17%) and also in all the provinces of the study area, including SC (77.48% *vs.* 22.52%), SAX (68.64% *vs.* 31.36%), SX (58.71% *vs.* 41.29%), HB (66.93% *vs.* 33.07%), GS (87.87% *vs.* 12.13%), IM (64.96% *vs.* 35.04%), NX (80.00% *vs.* 20.00%), QH (86.87% *vs.*13.13%), TB (69.45% *vs.* 30.55%), and XJ (79.00% *vs.* 21.00%). Thus, the impact of HA on grassland degradation was also larger than that of CC.

4. Discussion

4.1. Quantitative methods for assessing the contributions of climatic and human factors to grassland productivity

There have been relatively few quantitative analyses of the climatic and human factors that influence grassland productivity in northern China. Quantitatively evaluating the relative contributions of CC and HA to grassland productivity is a challenging task, whereas this is necessary for identifying the driving factors of grassland productivity. In view of this, this study tried to choose the NPP as an evaluation indicator of grassland productivity and differentiate the impact of CC on NPP changes from those of HA. A method based on partial derivatives was used to assess the contributions of climatic factors to NPP changes, and the difference between the inter-annual variation rate of NPP and the contributions from climatic factors was considered to be the impact of HA. Furthermore, different scenarios, which divided the complex driving mechanisms into simpler ones, were designed according to the relationship between grassland productivity and its driving forces from CC and HA. The method employed in this study is superior to mathematical statistical methods because it can distinguish the contributions of climatic and human factors to grassland productivity and be used to obtain the differences in the spatial distributions of these contributions. This method is also superior to the RESTREND method because NPP dynamics are sensitive to both CC and HA (Schimel, 1995; Zhou et al., 2014), so its application is not restricted by geographical conditions. Moreover, this method is superior to those based on potential and actual NPP because the uncertainty of simulated potential NPP can be avoided, and to some extent the contribution of single driving factor associated with CC and HA can be obtained. Therefore, this method

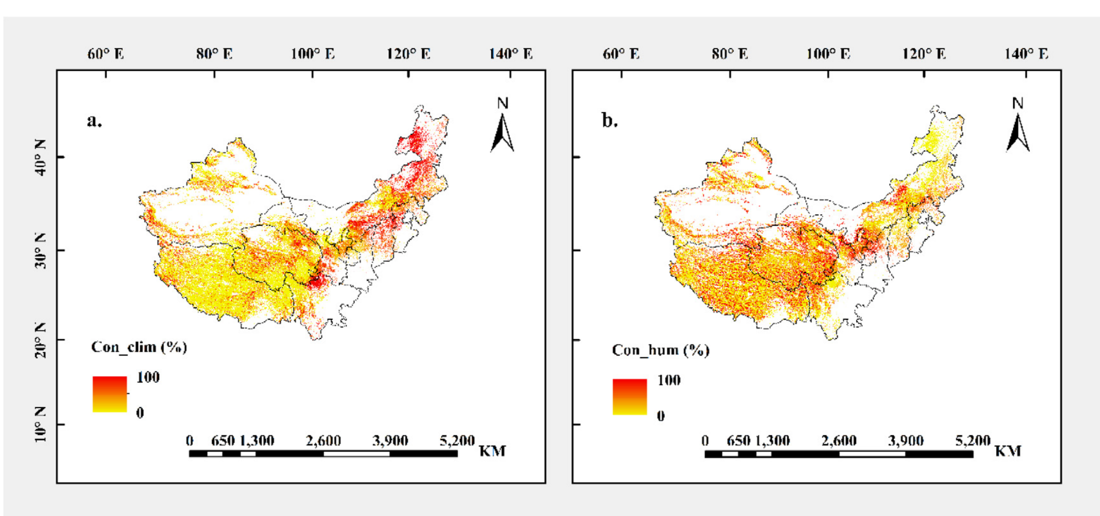

Fig. 9. Spatial distributions of the contribution proportions of (a) CC (Con_clim) and (b) HA (Con_hum) to grassland restoration.

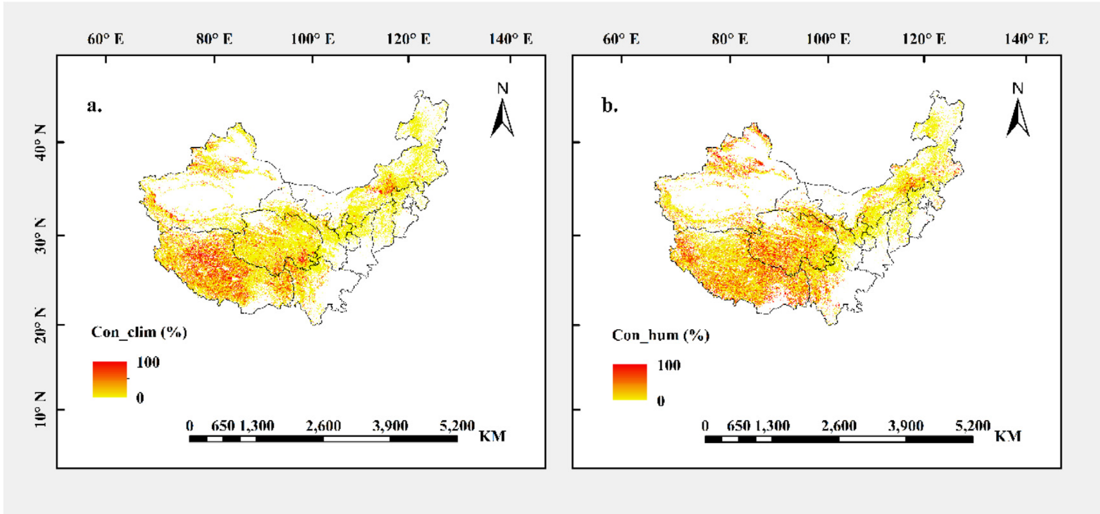

Fig. 10. Spatial distributions of the contribution proportions of (a) CC (Con_clim) and (b) HA (Con_hum) to grassland degradation.

provides a new way to quantitatively evaluate the contributions of climatic and human factors to grassland productivity.

4.2. Impact of CC on grassland productivity

Solar radiation made a greater positive contribution to grassland NPP changes than temperature or precipitation in northern China and also in most provinces (i.e., SC, SAX, SX, HB, GS, and XJ); this was likely because of the increasing trend of solar radiation in the majority of the study area (Fig. 13c), which increased the content of chlorophyll in plant leaves and in turn intensified photosynthesis and improved the rate of carbon sequestration in plants (Bonan, 2015; Kim et al., 2008; Liu et al., 2018; Li et al., 2017). Among the different provinces, precipitation made the greatest positive contribution to grassland NPP changes in IM; this may because grass growth is mostly restricted by precipitation in IM (Hao et al., 2014; Liu et al., 2014), and thus the increasing trend of precipitation in this province, especially in the east (Fig. 13b), could greatly promote grass growth. Solar radiation made the greatest positive contribution to grassland NPP changes in SX; this may because the amount of solar radiation in SX can scarcely meet the demands of grass growth (Wu et al., 2015; Yan et al., 2018; Liu et al., 2017), and thus the substantial increase of solar radiation in the majority of SX (Fig. 13c) could also greatly facilitate grass growth. Conversely, precipitation and solar radiation made the greatest negative contribution to grassland NPP changes in TB and QH, respectively; this may because precipitation in the majority of TB (Fig. 13b) and solar radiation in the whole QH (Fig. 13c) show decreasing trends.

Overall, the contribution of CC to grassland NPP changes was positive and much greater than that of HA in northern China. This finding is consistent with that of Zhu et al. (2007), who indicated that CC was favorable for vegetation growth in the Chinese mainland. However, CC had a negative influence on grassland NPP changes in some local regions such as the central part of TB (Fig. 8a), which is where CC was the dominant factor for grassland degradation (Figs. 10a and 11b). This is because precipitation decreased in this region, whereas temperature increased (Fig. 13a and b); i.e., the warmer and drier climates hindered vegetation growth (Cui and Graf, 2009). Our study also showed that among all provinces of the study area, both temperature and precipitation made the greatest negative contributions to grassland NPP changes in TB.

4.3. Impact of HA on grassland productivity

CC is an intrinsic driver of ecosystem change, and HA is an external driver that can strengthen or mitigate the influences of CC on ecosystems (Wang et al., 2006; Zheng et al., 2006; Zhou et al., 2014). HA,

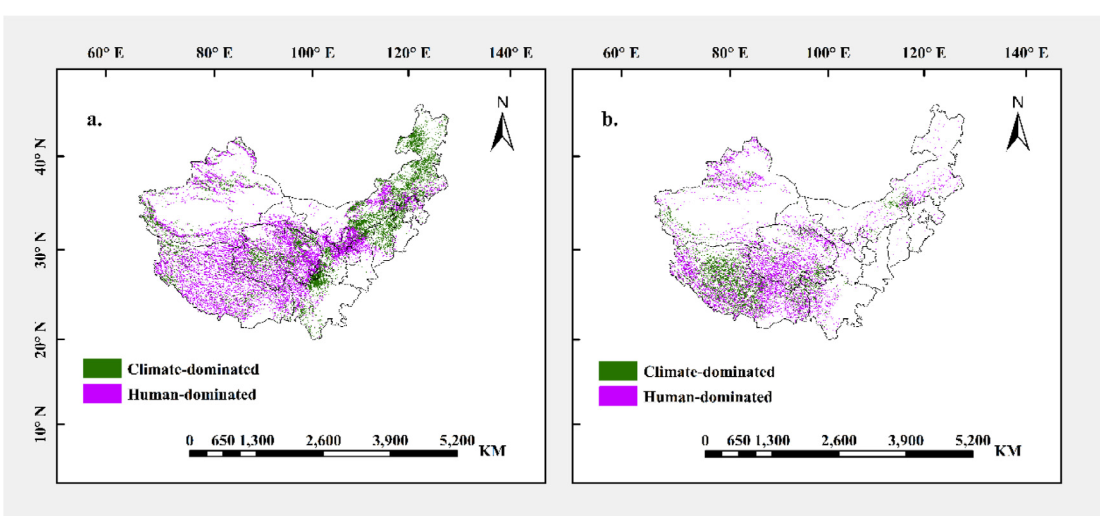

Fig. 11. Spatial distributions of the climate- and human-dominated (a) grassland restoration areas and (b) grassland degradation areas.

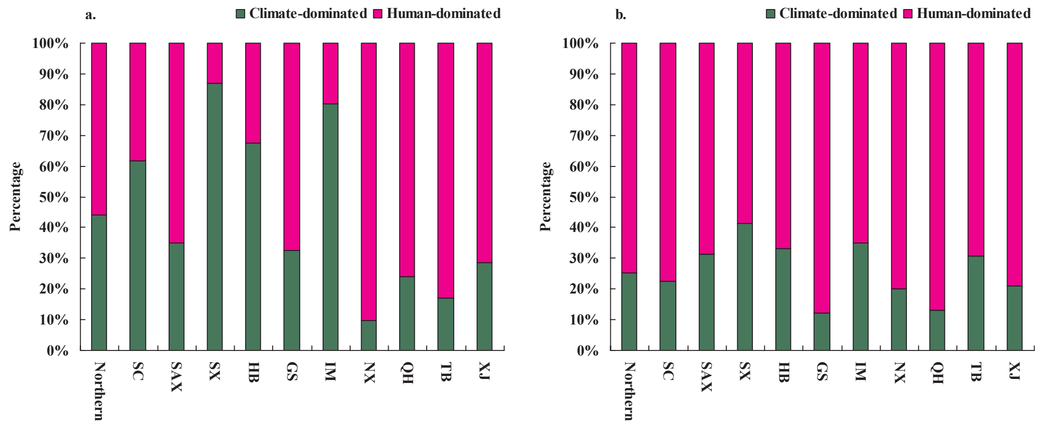

Fig. 12. Statistical analysis of the percentages of climate- and human-dominated (a) grassland restoration and (b) grassland degradation. See Fig. 1 for definitions of each province abbreviation.

such as overgrazing, conversion of grassland to cropland, illegal collection of wild medicinal materials, and unreasonable exploitation and use of water resources (Akiyama and Kawamura, 2007; Zhou et al., 2015; Zhou et al., 2017), can lead to grassland degradation. Our study found that HA played a major role in grassland degradation in northern China and in all provinces. This finding is in agreement with that of Zhou et al. (2014), who indicated that the dominant factor driving grassland degradation in the northwest China was HA.

However, in recent years, several ecological restoration projects, especially the GTGP and GWP, have been launched by the Chinese government to alleviate grazing pressure in degraded grassland areas. In general, these ecological protection policies have facilitated

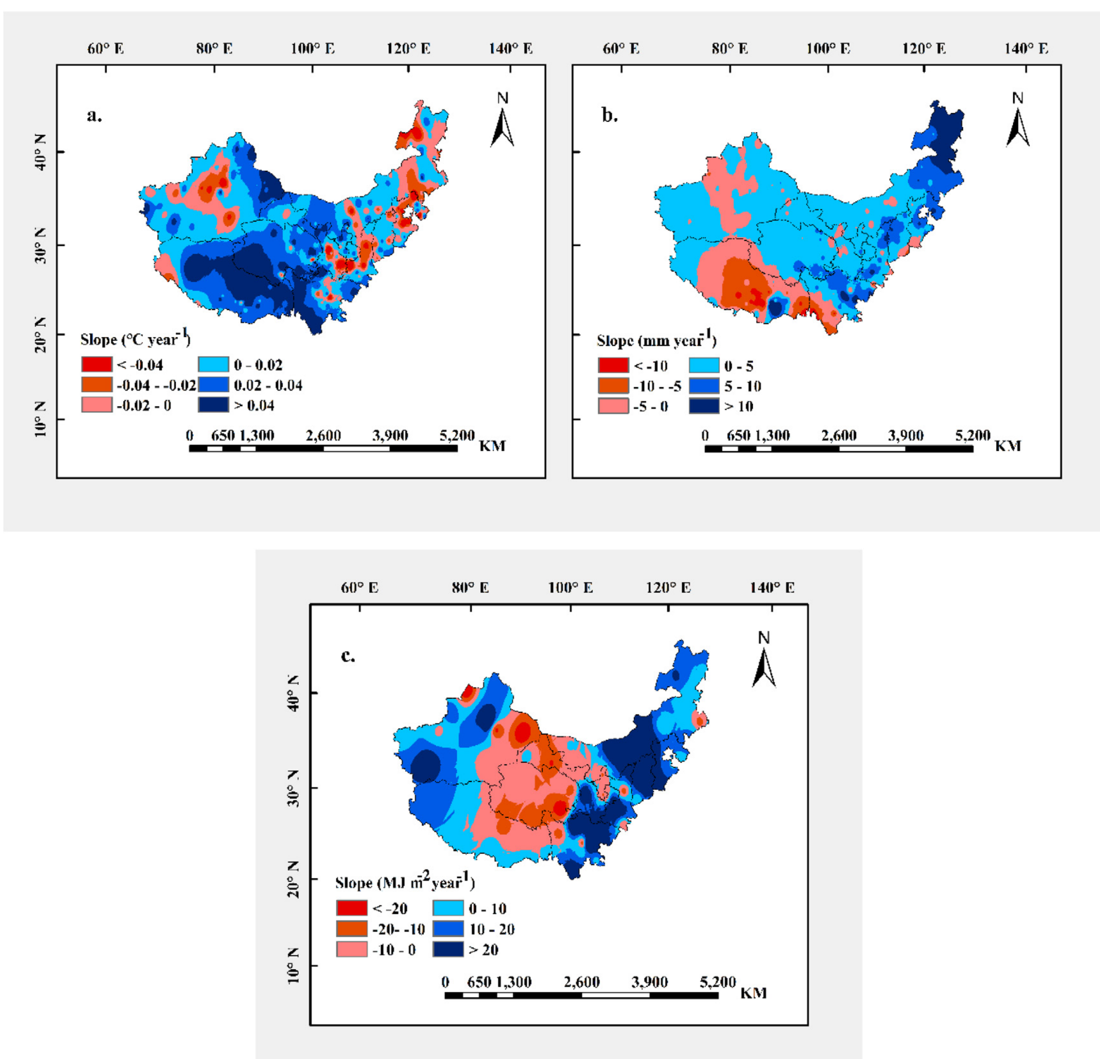

Fig. 13. Spatial distributions of the change trends in (a) temperature, (b) precipitation, and (c) solar radiation.

grassland restoration. For example, Bagan et al. (2010) reported that sparse grass areas increased due to implementation of the GTGP, and sand areas were successfully suppressed in Horqin sandy land. Wang et al. (2009) indicated that the GWP was beneficial for grassland restoration in Maqu County, Gansu province, and the effect of banning grazing was better than that of rest grazing. Our study showed that the contributions of HA to grassland NPP changes were positive in northern China and also in most provinces (i.e., SAX, SX, HB, GS, IM, NX, QH, and XJ). Moreover, HA played a major role in grassland restoration in northern China and also in most provinces (i.e., SAX, GS, NX, QH, TB, and XJ), which also demonstrated that these ecological restoration projects had positive effects on grassland productivity. It is worth noting that HA made the greatest positive contribution to grassland productivity in SAX (5.89 $g\,C\,m^{-2}\,year^{-1}$) among all provinces in the study area. This suggests that the GTGP and GWP have achieved remarkable results in the Loess Plateau, which is the pride of the Chinese people.

In our study, the impacts of HA on both grassland restoration and degradation were larger than those of CC in northern China; thus, the positive effect of HA on grassland productivity was substantially offset by its negative effect, which led to the positive contribution of HA to grassland NPP changes (0.58 $g\,C\,m^{-2}\,year^{-1}$) being smaller than that of CC (1.08 $g\,C\,m^{-2}\,year^{-1}$). Even worse, in the SC, HA made a negative contribution to grassland NPP changes ($-0.20\,g\,C\,m^{-2}\,year^{-1}$). Thus, our results reveal that the effective measures and policies to protect grassland resources should be further enhanced.

4.4. Limitations

In this study, a methodology that can be used to quantitatively evaluate the contributions of climatic and human factors to grassland productivity was designed by selecting NPP as the evaluation indicator. However, the limitations of this study should also be recognized. First, the results of this study were not verified by experimental data. Second, determining the contributions of some individual factors such as CO_2 fertilization, overgrazing, GTGP, and GWP to grassland productivity require further research. Therefore, the researches that focus on quantifying the influences of climatic and human factors more accurately and establishing a quantitative method of isolating the contributions of different human factors need to be further explored. Third, the scale represents the temporal and spatial dimensions that is used for measuring ecological processes (Prince, 2002; Verburg and Chen, 2000). The relationship between grassland productivity and its driving forces at one scale may not be applicable to another scale (Xu et al., 2010). Thus, the research that assesses the contributions of CC and HA to grassland NPP changes at a higher spatial resolution and a long-term scale by fusing multi-source data will be a better try in the future work.

5. Conclusion

In this study, we employed NPP as an evaluation indicator of grassland productivity and assessed the relative contributions of climatic and human factors to NPP changes in northern China. This method was shown to be superior to previous methods used to quantitatively evaluate the contributions of CC and HA to ecosystems. Furthermore, it enabled us to distinguish the contribution of single driving factor associated with CC and HA and determine the differences in the spatial distributions of these contributions. From 2000 to 2015, a significant increasing trend (1.66 $g\,C\,m^{-2}\,year^{-1}$, $P < 0.001$) was observed for grassland NPP in northern China. During this period, 64.94% of the grassland area exhibited an increasing trend in NPP, whereas 35.06% of the grassland area exhibited a decreasing trend. Moreover, temperature, precipitation, and solar radiation made positive contributions to grassland NPP changes in northern China, of which solar radiation made the greatest contribution, followed by precipitation and then temperature. The contributions of CC and HA to grassland NPP changes were 1.08 and 0.58 $g\,C\,m^{-2}\,year^{-1}$, respectively. CC thus made a greater positive contribution to grassland NPP changes than HA in northern China. The contributions of temperature, precipitation, solar radiation, CC, and HA to grassland NPP changes showed great spatial heterogeneity in the different provinces of northern China.

Regarding grassland restoration, two outcomes were observed in different provinces of northern China. First, CC played a major role in SC, SX, HB, and IM. Second, HA played a dominate role in SAX, GS, NX, QH, TB, and XJ. Regarding grassland degradation, the impacts of HA were larger than those of CC in all provinces. Overall, HA was the dominant factor affecting both grassland restoration and degradation in northern China. The negative effect of HA on grassland productivity greatly offsets its positive effect, and therefore more effective measures should be implemented to control grassland degradation in this region.

Acknowledgements

This work was funded by the National Key R & D Program of China (Grant No. 2017YFA0604404), and the National Natural Science Foundation of China (Grant No. 41671398, 41801304).

Appendix A. Supplementary data

Supplementary data to this article can be found online at https://doi.org/10.1016/j.ecolind.2019.04.020.

References

Akiyama, T., Kawamura, K., 2007. Grassland degradation in China: methods of monitoring, management and restoration. Grassl. Sci. 53 (1), 1–17.
Bagan, H., Takeuchi, W., Kinoshita, T., Bao, Y., Yamagata, Y., 2010. Land cover classification and change analysis in the Horqin Sandy Land from 1975 to 2007. IEEE J.-STARS. 3 (2), 168–177.
Bonan, G., 2015. Ecological Climatology: Concepts and Applications. Cambridge University Press.
Chen, Z., Wang, S., 2000. Typical Grassland Ecosystem in China. Science Press, Beijing.
Chen, B., Zhang, X., Tao, J., Wu, J., Wang, J., Shi, P., Zhang, Y., Yu, C., 2014. The impact of climate change and anthropogenic activities on alpine grassland over the Qinghai-Tibet Plateau Agric. For. Meteorol. 189, 11–18.
Chen, Y., Mu, S., Sun, Z., Gang, C., Li, J., Padarian, J., Li, S., 2016. Grassland carbon sequestration ability in China: a new perspective from terrestrial aridity zones. Rangeland Ecol. Manage. 69 (1), 84–94.
Cui, X., Graf, H.F., 2009. Recent land cover changes on the Tibetan Plateau: a review. Clim. Change 94 (1–2), 47–61.
Costanza, R., d'Arge, R., De Groot, R., Farber, S., Grasso, M., Hannon, B., Raskin, R.G., 1997. The value of the world's ecosystem services and natural capital. Nature 387 (6630), 253.
Du, X., Jin, X., Yang, X., Yang, X., Zhou, Y., 2014. Spatial pattern of land use change and its driving force in Jiangsu Province. Int. J. Environ. Res. Pub. Health 11 (3), 3215–3232.
Fang, J.Y., Guo, Z.D., Piao, S.L., Chen, A.P., 2007. Terrestrial vegetation carbon sinks in China, 1981–2000. Sci China: Earth Sci. 50 (9), 1341–1350.
Fang, Y.P., 2013. Managing the Three-Rivers Headwater Region, China: from ecological engineering to social engineering. Ambio 42 (5), 566–576.
Field, C.B., Behrenfeld, M.J., Randerson, J.T., Falkowski, P., 1998. Primary production of the biosphere: integrating terrestrial and oceanic components. Science 281 (5374), 237–240.
Gollnow, F., Lakes, T., 2014. Policy change, land use, and agriculture: the case of soy production and cattle ranching in Brazil, 2001–2012. Appl. Geogr. 55, 203–211.
Hao, L., Sun, G., Liu, Y., Gao, Z., Wu, B., 2014. Effects of precipitation on grassland ecosystem restoration under grazing exclusion in Inner Mongolia, China. Landscape Ecol. 29 (10), 1657–1673.
Harris, R.B., 2010. Rangeland degradation on the Qinghai-Tibetan plateau: a review of the evidence of its magnitude and causes. J. Arid Environ. 74 (1), 1–12.
Herrmann, S.M., Anyamba, A., Tucker, C.J., 2005. Recent trends in vegetation dynamics in the African Sahel and their relationship to climate. Glob. Environ. Change 15 (4), 394–404.
Huang, L., He, B., Chen, A., Wang, H., Liu, J., Lű, A., Chen, Z., 2016. Drought dominates the interannual variability in global terrestrial net primary production by controlling semi-arid ecosystems. Sci. Rep. 6, 24639.
Jiang, L., Bao, A., Guo, H., Ndayisaba, F., 2017. Vegetation dynamics and responses to climate change and human activities in Central Asia. Sci. Total. Environ. 599, 967–980.
Joos, F., Prentice, I.C., Sitch, S., Meyer, R., Hooss, G., Plattner, G.K., Hasselmann, K., 2001. Global warming feedbacks on terrestrial carbon uptake under the Intergovernmental Panel on Climate Change (IPCC) emission scenarios. Glob. Biogeochem. Cycle 15 (4), 891–907.

Kang, L., Han, X., Zhang, Z., Sun, O.J., 2007. Grassland ecosystems in China: review of current knowledge and research advancement. Philos. Trans. R. Soc. B-Biol. Sci. 362, 997–1008.
Keenan, T.F., Baker, I., Barr, A., Ciais, P., Davis, K., Dietze, M., Hufkens, K., 2012. Terrestrial biosphere model performance for inter-annual variability of land-atmosphere CO_2 exchange. Glob. Change Biol. 18 (6), 1971–1987.
Kim, J.H., Moon, Y.R., Wi, S.G., Kim, J.S., Lee, M.H., Chung, B.Y., 2008. Differential radiation sensitivities of Arabidopsis plants at various developmental stages. In: Photosynthesis. Energy from the Sun. Springer, Dordrecht, pp. 1491–1495.
Li, Q., Zhang, C., Shen, Y., Jia, W., Li, J., 2016. Quantitative assessment of the relative roles of climate change and human activities in desertification processes on the Qinghai-Tibet Plateau based on net primary productivity. Catena 147, 789–796.
Li, X., Chen, G., Liu, X., Liang, X., Wang, S., Chen, Y., Xu, X., 2017. A new global land-use and land-cover change product at a 1-km resolution for 2010 to 2100 based on human–environment interactions. Ann. Assoc. AM. Geogr. 107 (5), 1040–1059.
Liu, X., Hu, G., Chen, Y., Li, X., Xu, X., Li, S., Wang, S., 2018. High-resolution multi-temporal mapping of global urban land using Landsat images based on the Google Earth Engine Platform. Rem. Sens. Environ. 209, 227–239.
Liu, Y., Yang, Y., Wang, Q., Du, X., Li, J., Gang, C., Wang, Z., 2019. Evaluating the responses of net primary productivity and carbon use efficiency of global grassland to climate variability along an aridity gradient. Sci. Total. Environ. 652, 671–682.
Liu, X., Liang, X., Li, X., Xu, X., Ou, J., Chen, Y., Pei, F., 2017. A future land use simulation model (FLUS) for simulating multiple land use scenarios by coupling human and natural effects. Landscape. Urban. Plan. 168, 94–116.
Liu, W., Sun, F., 2016. Assessing estimates of evaporative demand in climate models using observed pan evaporation over China. J. Geophys. Res. Atmos. 121 (14), 8329–8349.
Liu, X., Ma, L., Li, X., Ai, B., Li, S., He, Z., 2014. Simulating urban growth by integrating landscape expansion index (LEI) and cellular automata. Int. J. Geogr. Inf. Sci. 28 (1), 148–163.
Lieth, H., Whittaker, R.H., 2012. Primary productivity of the biosphere. Springer Science & Business Media.
Mao, D., Wang, Z., Li, L., Song, K., Jia, M., 2014. Quantitative assessment of human-induced impacts on marshes in Northeast China from 2000 to 2011. Ecol. Eng. 68, 97–104.
Meng, D., Mo, X., 2012. Assessing the effect of climate change on mean annual runoff in the Songhua River basin, China. Hydrol. Process. 26 (7), 1050–1061.
Mu, Q., Zhao, M., Running, S.W., Liu, M., Tian, H., 2008. Contribution of increasing CO_2 and climate change to the carbon cycle in China's ecosystems. J. Geophys. Res. Biogeosci. 113.
Nan, Z., 2005. The grassland farming system and sustainable agricultural development in China. Grassl. Sci. 51 (1), 15–19.
Newman, M.E., McLaren, K.P., Wilson, B.S., 2014. Long-term socio-economic and spatial pattern drivers of land cover change in a Caribbean tropical moist forest, the Cockpit Country, Jamaica. Agric. Ecosyst. Environ. 186, 185–200.
Pei, F., Li, X., Liu, X., Wang, S., He, Z., 2013. Assessing the differences in net primary productivity between pre-and post-urban land development in China. Agric. Forest Meteorol. 171, 174–186.
Peng, S., Piao, S., Ciais, P., Myneni, R.B., Chen, A., Chevallier, F., Vicca, S., 2013. Asymmetric effects of daytime and night-time warming on Northern Hemisphere vegetation. Nature 501 (7465), 88.
Potter, C.S., et al., 1993. Terrestrial ecosystem production: a process model based on global satellite and surface data. Glob. Biogeochem. Cycle 7 (4), 811–841.
Prince, S.D., 2002. Spatial and temporal scales for detection of desertification. In: Global Desertification: Do Humans Cause Deserts, pp. 23–40.
Roderick, M.L., Rotstayn, L.D., Farquhar, G.D., Hobbins, M.T., 2007. On the attribution of changing pan evaporation. Geophys. Res. Lett. 34 (17).
Schimel, D.S., 1995. Terrestrial biogeochemical cycles: global estimates with remote sensing. Remote Sens. Environ. 51, 49–56.
Schweizer, P.E., Matlack, G.R., 2014. Factors driving land use change and forest distribution on the coastal plain of Mississippi, USA. Landsc. Urban Plan. 121, 55–64.
Scurlock, J.M.O., Hall, D.O., 1998. The global carbon sink: a grassland perspective. Glob. Change Biol. 4 (2), 229–233.
Verburg, P.H., Chen, Y., 2000. Multiscale characterization of land-use patterns in China. Ecosystems 3 (4), 369–385.
Wang, J., Guo, N., Cai, D.H., Deng, Z.Y., 2009. The effect evaluation of the program of restoring grazing to grasslands in Maqu County. Acta Ecol. Sin. 29, 1276–1284.
Wang, X., Chen, F., Dong, Z., 2006. The relative role of climatic and human factors in desertification in semiarid China. Glob. Environ. Change 16 (1), 48–57.
Wang, Z., Zhang, Y., Yang, Y., Zhou, W., Gang, C., Zhang, Y., Qi, J., 2016. Quantitative assess the driving forces on the grassland degradation in the Qinghai-Tibet Plateau, in China. Ecol. Inform. 33, 32–44.
Wen, Y., Liu, X., Pei, F., Li, X., Du, G., 2018. Non-uniform time-lag effects of terrestrial vegetation responses to asymmetric warming. Agric. Forest Meteorol. 252, 130–143.
Wessels, K.J., Prince, S.D., Malherbe, J., Small, J., Frost, P.E., VanZyl, D., 2007. Can human-induced land degradation be distinguished from the effects of rainfall variability? A case study in South Africa. J. Arid Environ. 68 (2), 271–297.
Wu, Y., Wu, Z., 2018. Quantitative assessment of human-induced impacts based on net primary productivity in Guangzhou, China. Environ. Sci. Pollut. 25 (12), 11384–11399.
Wu, D., Zhao, X., Liang, S., Zhou, T., Huang, K., Tang, B., et al., 2015. Time-lag effects of global vegetation responses to climate change. Glob. Change Biol. 21 (9), 3520.
Xu, D.Y., Kang, X.W., Zhuang, D.F., Pan, J.J., 2010. Multi-scale quantitative assessment of the relative roles of climate change and human activities in desertification–a case study of the Ordos Plateau, China. J. Arid Environ. 74 (4), 498–507.
Xu, J.H., 2006. Quantitative Geography. Higher Education Press.
Yang, H., Yang, D., 2012. Climatic factors influencing changing pan evaporation across China from 1961 to 2001. Jou. Hydrol. 414, 184–193.
Yan, Y., Liu, X., Ou, J., Li, X., Wen, Y., 2018. Assimilating multi-source remotely sensed data into a light use efficiency model for net primary productivity estimation. Int. J. Appl. Earth Obs. Geoinf. 72, 11–25.
You, G., Zhang, Y., Liu, Y., Song, Q., Lu, Z., Tan, Z., Xie, Y., 2013. On the attribution of changing pan evaporation in a nature reserve in SW China. Hydrol. Process. 27 (18), 2676–2682.
Zhang, Y., Zhang, C., Wang, Z., Chen, Y., Gang, C., An, R., Li, J., 2016. Vegetation dynamics and its driving forces from climate change and human activities in the Three-River Source Region, China from 1982 to 2012. Sci. Total. Environ. 563, 210–220.
Zhang, Z.B., 2003. Grassland rodent damage and management strategy. Bull. Chin. Acad. Sci. 5, 343–347.
Zheng, Y.R., Xie, Z.X., Robert, C., Jiang, L.H., Shimizu, H., 2006. Did climate drive ecosystem change and induce desertification in Otindag sandy land, China over the past 40 years? J. Arid Environ. 64 (3), 523–541.
Zhou, W., Gang, C., Zhou, L., Chen, Y., Li, J., Ju, W., Odeh, I., 2014. Dynamic of grassland vegetation degradation and its quantitative assessment in the northwest China. Acta Oecol. 55, 86–96.
Zhou, W., Gang, C., Zhou, F., Li, J., Dong, X., Zhao, C., 2015. Quantitative assessment of the individual contribution of climate and human factors to desertification in northwest China using net primary productivity as an indicator. Ecol. Indic. 48, 560–569.
Zhou, W., Yang, H., Huang, L., Chen, C., Lin, X., Hu, Z., Li, J., 2017. Grassland degradation remote sensing monitoring and driving factors quantitative assessment in China from 1982 to 2010. Ecol. Indic. 83, 303–313.
Zhu, W., Pan, Y., Yang, X., Song, G., 2007. Impact of climate change on net primary productivity of China's terrestrial vegetation. Chin. Sci. Bull. 52 (21), 2535–2541.